

Research paper

Cerebellar microstructural abnormalities in bipolar depression and unipolar depression: A diffusion kurtosis and perfusion imaging study



Lianping Zhao ^{a,b,1}, Ying Wang ^{a,c,1}, Yanbin Jia ^d, Shuming Zhong ^d, Yao Sun ^a, Zhifeng Zhou ^a, Zhongping Zhang ^e, Li Huang ^{a,*}

^a Medical Imaging Center, First Affiliated Hospital of Jinan University, Guangzhou 510630, China

^b Department of Radiology, Gansu Provincial Hospital, Gansu 730000, China

^c Clinical Experimental Center, First Affiliated Hospital of Jinan University, Guangzhou 510630, China

^d Department of Psychiatry, First Affiliated Hospital of Jinan University, Guangzhou 510630, China

^e General Electric Healthcare, Shanghai, 200000, China

ARTICLE INFO

Article history:

Received 29 October 2015

Received in revised form

21 December 2015

Accepted 26 January 2016

Available online 28 January 2016

Keywords:

Bipolar disorder

Unipolar depression

Diffusional kurtosis imaging

Perfusion imaging

Cerebellum

ABSTRACT

Background: Depression in the context of bipolar disorder (BD) is often misdiagnosed as unipolar depression (UD), leading to mistreatment and poor clinical outcomes. However, little is known about the similarities and differences in cerebellum between BD and UD.

Methods: Patients with BD ($n=35$) and UD ($n=30$) during a depressive episode as well as 40 healthy controls underwent diffusional kurtosis imaging (DKI) and three dimensional arterial spin labeling (3D ASL). The DKI parameters including mean kurtosis (MK), axial kurtosis (Ka), radial kurtosis (Kr), fractional anisotropy (FA), mean diffusivity (MD), axial diffusivity (Da) and radial diffusivity (Dr) and 3D ASL parameters (i.e. cerebral blood flow) was measured by using regions-of-interest (ROIs) analysis in the superior cerebellar peduncles (SCP), middle cerebellar peduncles (MCP) and dentate nuclei (DN) of cerebellum.

Results: Patients with UD exhibited significant differences from controls for DKI measures in bilateral SCP and MCP and cerebral blood flow (CBF) in bilateral SCP and left DN. Patients with BD exhibited significant differences from controls for DKI measures in the right MCP and left DN and CBF in the left DN. Patients with UD showed significantly lower MD values compared with patients with BD in the right SCP. Correlation analysis showed there were negative correlations between illness duration and MD and Dr values in the right SCP in UD.

Limitations: This study was cross-sectional and the sample size was not large. Parts of the patients included were under medication prior to MRI scanning.

Conclusions: Our findings provide new evidence of microstructural changes in cerebellum in BD and UD. The two disorders may have overlaps in microstructural abnormality in MCP and DN during the depressive period. Microstructural abnormality in SCP may be a key neurobiological feature of UD.

© 2016 Elsevier B.V. All rights reserved.

1. Introduction

In patients with mood disorder, typical features are feeling sad all the time, losing interest in important parts of life, fluctuating between extreme happiness and extreme sadness (Cai et al., 2015). The most common mood disorders are bipolar disorder (BD) and unipolar depression (UD) (Davis and Gamble, 2015). Although BD consists of recurring episodes of mania and depression, the depressive episodes of BD are the most common mood manifestation

of the illness. Therefore, BD-II is often misdiagnosed as major depressive disorder or recurrent UD leading to inadequate treatment, huge medical costs and poor clinical outcomes (Bowden, 2010; Sasayama et al., 2011). However, consistent biomarkers distinguishing the disorders have been elusive. Accumulating evidence suggests a wide spread structural and functional brain abnormalities in patients with BD and UD (Kempton et al., 2011). But only a few neuroimaging studies have already been published directly comparing the two disorders.

The cerebellum has traditionally been regarded as a region which is mainly associated with coordination of voluntary movement, gait, posture, speech and motor function. However, evidences from literatures suggest a possible role of the cerebellum in cognition, mood and behavior (Rapoport et al., 2000; Schmahmann,

* Corresponding author. Tel.: +86 20 38688005; fax: +86 20 85228523.

E-mail addresses: johneil@vip.sina.com (Y. Wang), cjr.huangli@vip.163.com (L. Huang).

¹ Authors Lianping Zhao and Ying Wang are first co-authors.

2004). In recent years, published studies have indicated that the cerebellum plays an important role in the pathogenesis of BD and UD (Ambrosi et al., 2016; Arnold et al., 2012; Kim et al., 2013; Liang et al., 2013; Machino et al., 2014; Wang et al., 2015a). Structural neuroimaging showed a greater reduction in gray matter density (Kim et al., 2013) and volume (Machino et al., 2014) in the cerebellum, while functional neuroimaging found voxel-mirrored homotopic connectivity differences (Wang et al., 2015a) and regional homogeneity decreases (Liang et al., 2013) by use of resting-state fMRI in the two disorders. Furthermore, the cerebellum is identified as an important component of the neuronal circuitry that is connected to many regions of the cerebrum through the superior and middle cerebellar peduncles (SCP, MCP). It is a critical structure (including SCP, MCP and dentate nuclei) in the prefrontal-thalamic-cerebellar circuit which is related to both cognitive and affective functions (Buckner, 2013; Parker et al., 2013). This circuit has been found to be abnormal in patients with schizophrenia in structural (Rusch et al., 2007) and functional (Honey et al., 2005; Parker et al., 2013) neuroimaging studies. Nevertheless, far too little attention has been paid to this circuitry in BD and UD. Several studies have also found altered prefrontal-thalamic-cerebellar circuit regions in BD and UD, including the prefrontal cortex and thalamus (Chen et al., 2015; Guo et al., 2013a; McKenna et al., 2014; Redlich et al., 2015; Wang et al., 2015b), but only few studies have been done for cerebellum changes.

Recently, a relatively new diffusion imaging technique, diffusion kurtosis imaging (DKI), has been introduced and is increasingly being used for human brain studies. DKI characterizes non-Gaussian water diffusion behavior in neural tissues, whereas conventional diffusion tensor imaging (DTI) is limited to Gaussian diffusion (Jensen and Helpern, 2010; Lu et al., 2006). Non-Gaussian diffusion is believed to arise from diffusion barriers, such as cell membranes and organelles, and is therefore thought to be a sensitive indicator of tissue microstructural integrity. With DKI, both the apparent diffusion and apparent diffusional kurtosis are quantified. It has been shown that DKI can provide information additional to DTI that reflects the microstructure of the brain (Hui et al., 2008; Jensen et al., 2011; Lu et al., 2006), and hence can potentially improve the sensitivity and specificity of characterization of the neural tissues in human brain. In contrast to conventional DTI metrics, DKI is not limited to anisotropic environments, and thus permits the quantification of the microstructural integrity of both gray and white matter, even in the presence of crossing fibers (Lu et al., 2006). This sensitivity to gray matter may be of importance in the examination of the microstructural integrity in the brain. Based on DKI data, both kurtosis parameters such as mean kurtosis (MK), axial kurtosis(Ka) and radial kurtosis (Kr) and diffusion parameters including fractional anisotropy (FA), mean diffusivity (MD), axial diffusivity (Da) and radial diffusivity (Dr) could be obtained. It is worth noting that, due to the inclusion of non-Gaussian effects, the DKI derived estimates of the diffusion indices (FA, MD, Da and Dr) will generally be more accurate than those obtained with conventional DTI (Veraart et al., 2011). Since DKI first introduced by Jensen et al. (Jensen et al., 2005), it has shown promising preliminary results for several brain diseases including temporal lobe epilepsy (Bonilha et al., 2014), Parkinson disease (Kamagata et al., 2014), attention-deficit hyperactivity disorder (Helpern et al., 2011), as well as schizophrenia (Zhu et al., 2015). So far, however, there has been little study related to BD and UD by using DKI to evaluate the microstructure integrity of the cerebellum.

In the present study, we aimed to investigate the possible abnormalities of cerebellum in BD-II and UD by using DKI and three dimensional arterial spin labeling (3D ASL). We hypothesized that the two patient groups would share similarities and exhibit differences in microstructural and perfusional changes in the SCP,

MCP and dentate nuclei (DN) according to the prefrontal-thalamic-cerebellar circuit. To our best knowledge, this is the first study to show the changes in the cerebellum in the two disorders, which might help differentiate BD-II from UD depression.

2. Methods

2.1. Subjects

Thirty-five patients with depressed BD and 30 patients with UD were recruited from the in-patient unit of the psychiatry department, First Affiliated Hospital of Jinan University, Guangzhou, China. The patients were aged from 18 to 55 years. All participants met DSM-IV criteria based on the Structured Clinical Interview for DSM-IV Patient Edition (SCID-P) for BD and UD with a score 18 or greater on the 17-item Hamilton Depression Rating Scale (HDRS). Patients with other Axis-I psychiatric disorders, a history of organic brain disorder, neurological disorders, mental retardation, cardiovascular diseases, alcohol/substance abuse, pregnancy, or any physical illness were excluded from the study. None of the patients had ever received electroconvulsive therapy prior to participating in the study. At the time of the study, 20 patients in the BD group and 23 in the UD group were either medication-naïve or had been unmedicated for at least five months. The remaining patients with BD were receiving antidepressants (duloxetine or paroxetine), and/or mood stabilizers (lithium, sodium valproate), and/or atypical antipsychotic medications (olanzapine or risperidone). The remaining patients with UD were receiving antidepressants (duloxetine or paroxetine). The treatment duration for these BD and UD patients was no more than six weeks.

Forty-five healthy controls (HC) were recruited by local advertisements. They were carefully screened through a diagnostic interview, the Structured Clinical Interview for DSM- IV Nonpatient Edition (SCID-NP), to rule out the presence of current or past history of substance abuse/dependence or any psychiatric illness in self or in first-degree relatives. Further exclusion criteria for HC were any history of cerebrovascular disease, past head injury, epilepsy, migraine, hypertension, diabetes, and other types of disorders potentially affecting the central nervous system. All participants were right-handed and were submitted to MRI scanning within 48 h of initial contact. This study was conducted in accordance with the Declaration of Helsinki (1989) and was approved by the Ethics Committee of the First Affiliated Hospital of Jinan University, China. All participants signed informed consent form after a full written and verbal explanation of the study. Two senior clinical psychiatrists confirmed that all subjects had the ability to consent to participate in the examination.

2.2. MR techniques

Experiments were conducted on a 3 T MR system (Discovery MR 750 System, GE Healthcare, Milwaukee, WI, USA) with an 8-channel phased array head coil. Subjects were scanned in a supine, head-first position with symmetrically placed cushions on both sides of the head to decrease motion.

The DKI experiments were performed using a twice-refocused-spin-echo (TRSE) diffusion sequence with 15 different diffusion encoding directions using an optimized sampling strategy. For each direction, six b-values ($b=0, 500, 1000, 1500, 2000, 2500 \text{ s/mm}^2$) were used. Other imaging parameters were: TR = 4500 ms, TE = minimum, field of view (FOV) = $256 \times 256 \text{ mm}^2$, matrix = 128×128 , parallel imaging factor of 2 with 24 k-lines used as references, number of averages = 2, slice thickness = 2 mm, voxel size $2 \times 2 \times 2 \text{ mm}^3$. The total scan duration for the DKI sequence was 12 min 5 seconds. 3D ASL was performed by use of a

pseudocontinuous arterial spin labeling (pCASL) period of 1500 ms with a post labeling delay time of 1525 ms. TR=4632 ms, TE = 10.5 ms, FOV = 24 × 24 cm, slice thickness = 4 mm. Whole-brain images were obtained with an interleaved 3D stack of spirals fast spin echo (FSE) sequence and background suppression. Multiarm spiral imaging was used, with 8 arms and 1024 points acquired on each arm. A high level of background suppression was achieved by use of 4 separate inversion pulses spaced around the pseudo-continuous labeling pulse. The entire process took 4 min 29 sec to complete which included proton attenuation. In addition, a three dimensional brain volume imaging (3D BRAVO) sequence covering the whole brain was used for structural data acquisition with: TR/TE = 8.2 msec/3.2 msec, slice thickness = 1.0 mm, gap = 0 mm, matrix = 256 × 256, FOV = 24 × 24 cm, NEX = 1, flip angle = 12°, bandwidth = 31.25 Hz, acquisition time = 3 min 45 sec. Routine MRI examination images were also collected for excluding anatomic abnormality, such as T1 weighted, T2 weighted, diffusion-weighted imaging (DWI), and T2/fluid-attenuated inversion recovery (FLAIR) images. All participants were found, by two experienced radiologists, to have no abnormalities on routine MRI.

2.3. Data Processing

The data were transferred to a dedicated workstation (General Electric Advantage Workstation 4.5) where the DKI and 3D ASL data were post-processed using Functool software version 9.4.05a. The Functool program corrected echo planar imaging (EPI) distortion and eddy current. The diffusion and kurtosis tensors were calculated using the DKI model described previously by Jensen et al. (Jensen and Helpern, 2010; Jensen et al., 2005) which embedded in the Functool software. The key relationship is:

$$\ln[S(b)] = \ln[S(0)] - bD_{app} + \frac{1}{6}b^2D_{app}^2K_{app} + O(b)^3 \quad (1)$$

where $S(b)$ is the signal intensity at the echo time, D_{app} is the apparent diffusion coefficient, and K_{app} is the apparent diffusional kurtosis. The parameter b is given by the usual expression $(\gamma\delta g)^2(\Delta - \delta/3)$, where γ is the proton gyromagnetic ratio. In carrying out the expansion of equation [1], it is assumed that b is changed by varying the gradient strength g with the timing parameters δ and Δ being kept fixed. Just as D_{app} is an estimate for the diffusion coefficient in the direction parallel to the orientation of diffusion sensitizing gradients, K_{app} is an estimate for the diffusional kurtosis in this same direction (Jensen et al., 2005). With our DKI protocol, we obtained parametric maps related to diffusional kurtosis: MK, Ka and Kr. Conventional DTI-based metrics were also derived, including FA, MD, Da and Dr. Details for the computation of these metrics have been described previously (Jensen and Helpern, 2010; Lu et al., 2006).

The kinetic model for 3D ASL proposed by Alsop and Detre was used in this study (Alsop and Detre, 1996). Besides, we included a term for the finite labelling duration (Wang et al., 2005) and correct the incomplete recovery of the tissue signal in the reference image due to the saturation performed t_{sat} (2,000 ms) before imaging (Jarnum et al., 2010). The quantitative CBF maps were generated using the following equation (Jarnum et al., 2010; Wu et al., 2014):

$$CBF = \frac{\lambda \left(1 - e^{-\frac{t_{sat}}{T_{1g}}} \right)}{2\alpha T_{1b} \left(1 - e^{-\frac{t}{T_{1b}}} \right) S_0} \frac{\Delta S}{S_0} e^{\frac{\omega}{T_{1b}}} \quad (2)$$

where CBF is the cerebral blood flow; T_{1b} is the T_1 relaxation time of the blood (1600ms) in 3.0 T, T_{1g} represents the T_1 relaxation time of the gray matter (1200ms) in 3.0 T, t_{sat} is the duration time

of saturation pulse performed before imaging (2000ms), α is the labeling efficiency (0.8), λ is brain/blood partition coefficient (0.9), τ is the labeling duration(1500ms), ω is the postlabeling delay time (1525ms). The inversion slab is 22 mm below the acquired volume. Resolution of pCASL data is 3.7 mm (FOV 24 cm, reconstructed matrix: 64 × 64).

Regions of interest (ROIs) drawing methods were made based on Okugawa et al. and Xueying et al.'s ROIs analysis (Okugawa et al., 2006; Xueying et al., 2015) and determined by two independent neuroradiologists (LP.Z and Y.W, with 5 and 9 years of experience, respectively) who were blinded to the patient or control status. For each subject, DKI, 3D ASL and 3D BRAVO can fused with each other. ROIs manually placed in the bilateral SCP, MCP, and DN of the cerebellum on the maximum level of the structures. Considering the relatively low resolution of the DKI and CBF maps, we selected high resolution 3D BRAVO images to fuse with the DKI and CBF maps as the reference image. Separate ROIs were drew carefully according to the morphous of the SCP, MCP and DN (hypointense) on the b_0 images firstly, and then the 3D BRAVO images were used to minimize variation and better delineate the borders of the ROIs against surrounding structures. The ROIs of MCP also drawing according to the fibers of MCP shown in Dr map from DKI which is bluer than surrounding stuctures especially to avoid the inferior cerebellar peduncle in the inner side of MCP (Fig. 1a-f). For each subject, ROI sizes were identical in the left and right cerebellar hemispheres by using the mirror symmetry tools from the Functool software. However, the size of SCP, MCP and DN differed among the subjects, and thus the ROIs could not be the same. The areas in the SCP, MCP and DN ranged from 73 to 102 mm², from 168 to 212 mm² and from 106 to 155 mm² respectively. Major vascular structures and artefacts were avoided in placing the ROIs. All ROIs of DKI parameters were then transferred to the maps of MK, Ka, Kr, FA, MD, Da, and Dr (Fig. 2a-g, h-n and o-u) while the ROIs of 3D ASL were transferred to the maps of CBF (Fig. 3a-c) for measurement.

2.4. Statistical analysis

Statistical analyses were performed using SPSS for Windows software, version 17.0 (SPSS Inc., Chicago, and III, USA). Distributions of age and years of education between the three groups were compared with one-way analysis of variance (ANOVA). Chi-square test was used to compare gender distributions. ANOVA with Bonferroni's multiple comparison tests was performed to compare the DKI parameters and CBF values of all the three ROIs among BD ($n=35$), UD ($n=30$) and HC ($n=35$) groups respectively in the left and right cerebellar hemispheres and among the unmedicated BD ($n=20$), UD ($n=23$) and HC ($n=35$) subjects. If equal variances not assumed, use Tamhane's multiple comparison tests.

Pearson's correlation coefficients were used to correlate the clinical variables for the patients to their measured DKI and 3D ASL parameters. Inter-rater reliability was assessed using the intra-class correlation coefficient (ICC) analysis. A P -value of less than 0.05 was considered statistically significant.

3. Results

3.1. Demographic result

Table 1 shows the demographics and clinical data of all study participants. There was no significant difference between the three groups in age, gender and education levels of the subjects recruited for this study. These two depressed groups were matched for depression severity, illness duration, and illness onset age.

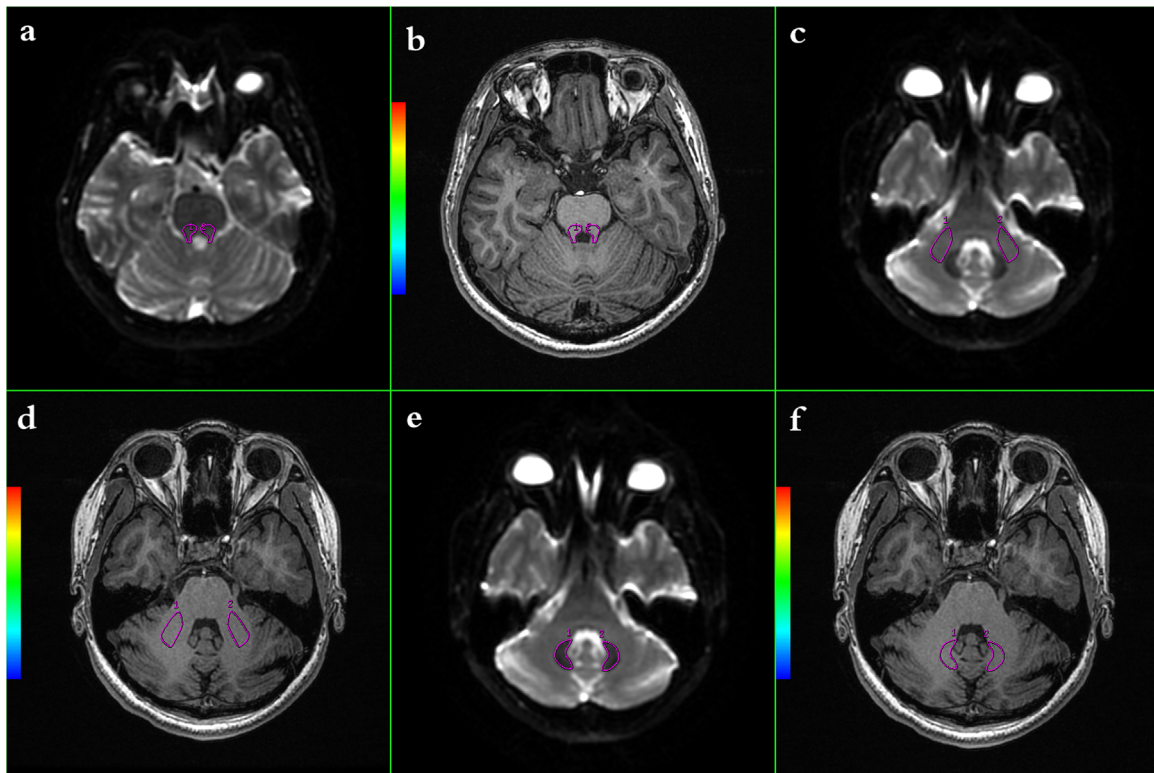


Fig. 1. **a-f.** Fig. 1a-b: ROIs of SCP on axial b0 image and high resolution 3D BRAVO image. Fig. 1c-d: ROIs of MCP on axial b0 image and high resolution 3D BRAVO image. Fig. 1e-f: ROIs of DN on axial b0 image and high resolution 3D BRAVO image.

3.2. Inter-rater reliability analysis

ICC analysis showed a significantly high value which was all greater than 0.70 in the three ROIs, and ICC value was close to 1 ($P < 0.05$). Hence, all measurements were regarded as reliable among different raters (Table 2). Therefore, averaged values were used for subsequent statistical analyses.

3.3. Group differences of the parameters generated from DKI

Table 3 shows the DKI parameters in the three groups (Fig. 4). In the SCP, ANOVA revealed significant differences in K_a , MD and D_r between the three groups. Post hoc comparisons revealed the UD group showed significantly increased K_a (left: $P=0.034$, right: $P=0.027$), MD (left: $P=0.003$, right: $P=0.023$) and decreased D_r (left: $P=0.006$, right: $P=0.035$) compared with the HC group. In addition, MD values were lower ($P=0.008$) in the UD group than in the BD group in the right SCP. In the MCP, ANOVA revealed significant differences in K_a , FA and D_r between the three groups. Post hoc comparisons revealed the UD group showed significantly increased K_a (left: $P=0.008$, right: $P=0.044$) and decreased FA (left: $P=0.027$, right: $P=0.020$) in bilateral MCP and increased D_r ($P=0.045$) in the right MCP compared with the HC group. The BD group showed significantly decreased FA ($P=0.001$) and increased D_r ($P=0.012$) in the right MCP compared with the HC group. In the DN, ANOVA revealed significant differences in M_K and K_a between the three groups. Post hoc comparisons revealed only the BD group showed significantly decreased M_K ($P=0.047$) in the left DN compared with the HC group. No significant changes in the remaining DKI parameters were observed in the three ROIs among the three groups.

The results of group differences of the DKI parameters in unmedicated patients with BD ($n=20$), UD ($n=23$) and HC ($n=35$) subjects were added in the supplemental information (Table S1).

3.4. Group differences in CBF

Table 4 shows the results of CBF in the three groups (Fig. 5). ANOVA revealed significant differences in bilateral SCP and the left DN between the three groups. Post hoc comparisons showed significantly decreased CBF in bilateral SCP (left: $P=0.028$, right: $P=0.045$) and the left DN ($P=0.020$) in the UD group compared with the HC group. And significantly decreased CBF in the left DN ($P=0.021$) in the BD group compared with the HC group. No significant changes in the rest of the CBF were observed in the three ROIs among the three groups.

The results of group differences of CBF in unmedicated patients with BD ($n=20$), UD ($n=23$) and HC ($n=35$) subjects were added in the supplemental information (Table S2).

3.5. Correlations between DKI/3D ASL parameters and HDRS-24 score/illness duration

Correlation analysis revealed a significant negative correlation between illness duration and MD ($r=-0.506$, $P=0.004$) and D_r values ($r=-0.604$, $P=0.000$) in the right SCP in the UD group (Fig. 6a-b). There were no significant correlations between the remaining DKI and 3D ASL parameters in these regions and the clinical variables (HDRS scores, illness duration) in the patients with either BD or UD.

4. Discussion

The current study, to our knowledge, is the first study to directly compare the difference in the microstructural organization of cerebellum in BD and UD depressed adults and healthy subjects by using DKI and 3D ASL. The two disorders showed similarities and differences in the microstructural and perfusional changes in the cerebellum. This study has several principal findings. First,

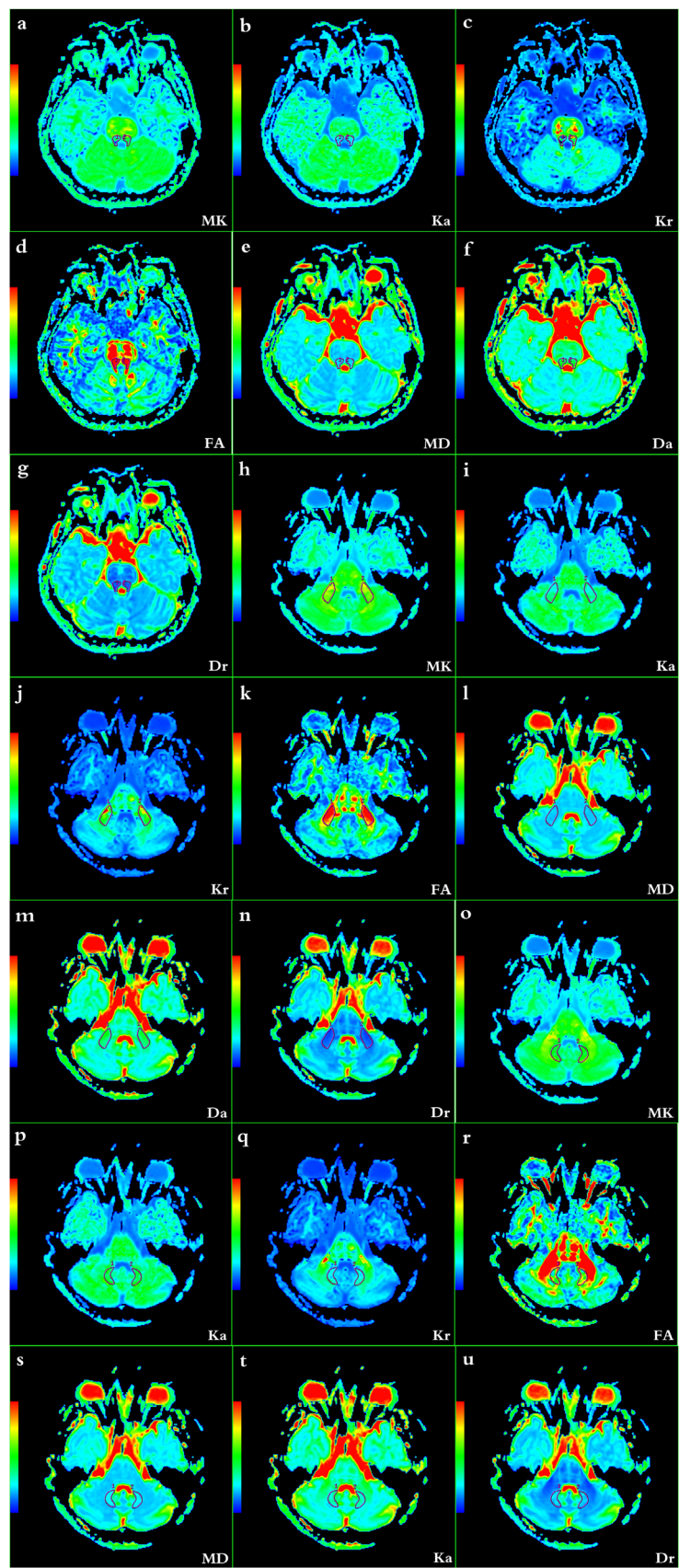


Fig. 2. **a-u.** ROIs of SCP (Fig. 2a-g), MCP (Fig. 2h-n) and DN (Fig. 2o-u) on corresponding MK, Ka, Kr, FA, MD, Da, Dr map.

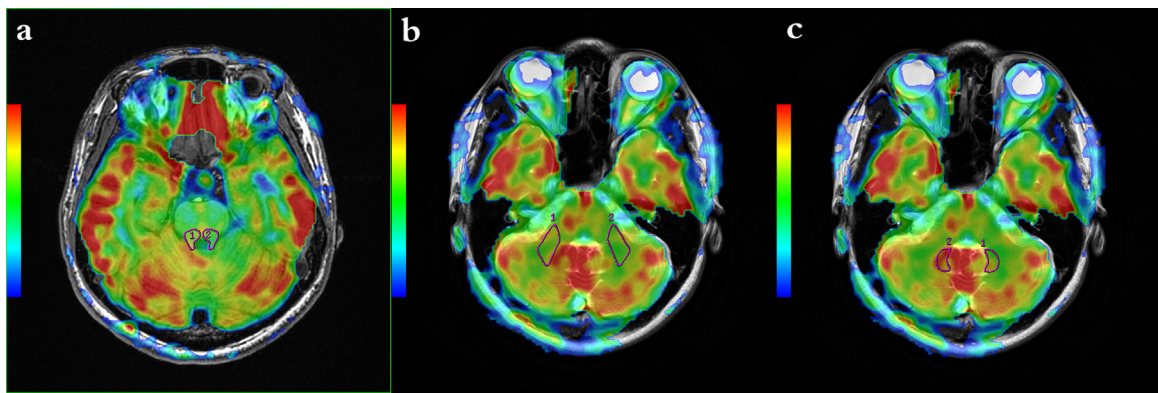


Fig. 3. a-c: ROIs of SCP, MCP and DN on CBF map which fused with 3D BRAVO (Fig. 3a) and T₂WI (Fig. 3b-c).

Table 1
The demographic characteristics of the subjects.

	BD n=35	UD n=30	HC n=45	Statistic
Gender(male/ female)	18/17	13/17	22/23	$\chi^2=0.439$ $P=0.803$
Age(years)	30.31 (10.07)	33.9 (9.28)	31.91(11.73)	$F=0.927$ $P=0.399$
Education(years)	13.31 (3.20)	12.94 (3.53)	14.43(3.05)	$F=2.526$ $P=0.084$
Duration of illness (months)	41.77 (39.56)	34.71 (52.28)	n/a	$t=0.643$ $P=0.522$
Age of illness Onset (years)	25.78 (9.11)	29.66 (12.72)	n/a	$t=1.444$ $P=0.154$
HDRS-24 score (points)	25.73 (5.36)	24.08 (6.14)	n/a	$t=-1.164$ $P=0.249$
YMRs score (points)	2.68 (1.15)	2.15 (1.22)	n/a	$t=-1.791$ $P=0.078$
Number of past manic/depressive episodes	2.02 (2.01)	3.26 (6.07)	n/a	n n

Values are reported as mean (standard deviation), except for gender. BD=bipolar disorder. UD=unipolar depression. HC=healthy controls. HDRS=Hamilton Depression Rating Scale. YMRS=Young Mania Rating Scale.

patients with UD exhibited microstructural abnormalities in bilateral SCP and MCP and decreased CBF in bilateral SCP and the left DN. Second, patients with BD exhibited microstructural abnormalities in the right MCP and the left DN and decreased CBF only in the left DN. Third, patients with UD showed significantly lower MD values compared with patients with BD in the right SCP. At

last, correlation analysis showed there were negative correlations between illness duration and MD and Dr values in the right SCP in UD.

In the present study, we observed increased Ka and decreased MD and Dr in bilateral SCP in UD but not in BD. In addition, patients with UD showed decreased MD compared with patients with BD in the right SCP. Da and Ka are believed to reflect axonal integrity while Dr and Kr are believed to reflect myelin integrity (Cheung et al., 2009; Hui et al., 2008; Song et al., 2002). MD corresponds to the average of the diffusion coefficient over all directions. Decreased MD may reflect increases of cellular density (Abe et al., 2010). Although the exact pathological process that occurs in SCP in patients with UD is still unknown, from the above theory, increased Ka (Helpert et al., 2011) and decreased MD and Dr indicated that water diffusion is more restricted and microstructure is changed in the SCP in UD compared with HC subjects. It may result from increased myelination, denser packing of axons and fiber bundles, changes in axonal membrane permeability. According to the results that MD values were lower in UD than in BD, we speculated that more denser cellular density was existed in the right SCP in UD. The SCP is a pivotal pathway which connects the cerebellar cortex and the deep cerebellar nuclei (include the DN) with the cerebrum. It has been demonstrated neural disorganization in schizophrenia in reviewing the literature (Okugawa et al., 2006). Okugawa G et al. reported significant lower FA in bilateral SCP in schizophrenia compared with healthy subjects. Meanwhile, the authors also found the FA abnormality was associated with cognitive abnormality (Okugawa et al., 2006). A recent resting-state functional MRI study by Guo W et al. found increased functional connectivity between the cerebellar and the prefrontal

Table 2
Inter-rater reliability of DKI and 3D ASL parameters in the SCP, MCP, and DN.

	MK		Ka		Kr		FA		MD		Da		Dr		CBF	
	L	R	L	R	L	R	L	R	L	R	L	R	L	R	L	R
SCP																
α	0.898	0.832	0.871	0.885	0.844	0.887	0.862	0.885	0.840	0.934	0.864	0.834	0.864	0.878	0.990	0.939
ICC	0.811	0.714	0.730	0.792	0.717	0.777	0.731	0.772	0.712	0.866	0.762	0.717	0.710	0.733	0.972	0.882
P	0.000	0.000	0.000	0.000	0.000	0.000	0.000	0.000	0.000	0.000	0.000	0.000	0.000	0.000	0.000	0.000
MCP																
α	0.954	0.944	0.939	0.878	0.958	0.934	0.863	0.971	0.861	0.965	0.924	0.867	0.986	0.965	0.885	0.864
ICC	0.898	0.854	0.846	0.745	0.807	0.835	0.704	0.914	0.714	0.899	0.773	0.731	0.910	0.847	0.795	0.762
P	0.000	0.000	0.000	0.000	0.000	0.000	0.000	0.000	0.000	0.000	0.000	0.000	0.000	0.000	0.000	0.000
DN																
α	0.942	0.947	0.868	0.877	0.908	0.905	0.943	0.901	0.930	0.901	0.902	0.918	0.954	0.935	0.992	0.993
ICC	0.885	0.899	0.764	0.752	0.829	0.826	0.885	0.817	0.869	0.821	0.823	0.846	0.912	0.877	0.982	0.983
P	0.000	0.000	0.000	0.000	0.000	0.000	0.000	0.000	0.000	0.000	0.000	0.000	0.000	0.000	0.000	0.000

MK=mean kurtosis. Ka= axial kurtosis. Kr= radial kurtosis. FA=fractional anisotropy. MD=mean diffusivity. Da=axial diffusivity. Dr= radial diffusivity. L=left. R=right. SCP=superior cerebellar peduncles. MCP= middle cerebellar peduncles. DN=dentate nuclei. α=Cronbach's alpha. ICC=intra-class correlation coefficient.

Table 3

Comparison of the DKI parameters of cerebellum in patients with BD, UD and HC subjects.

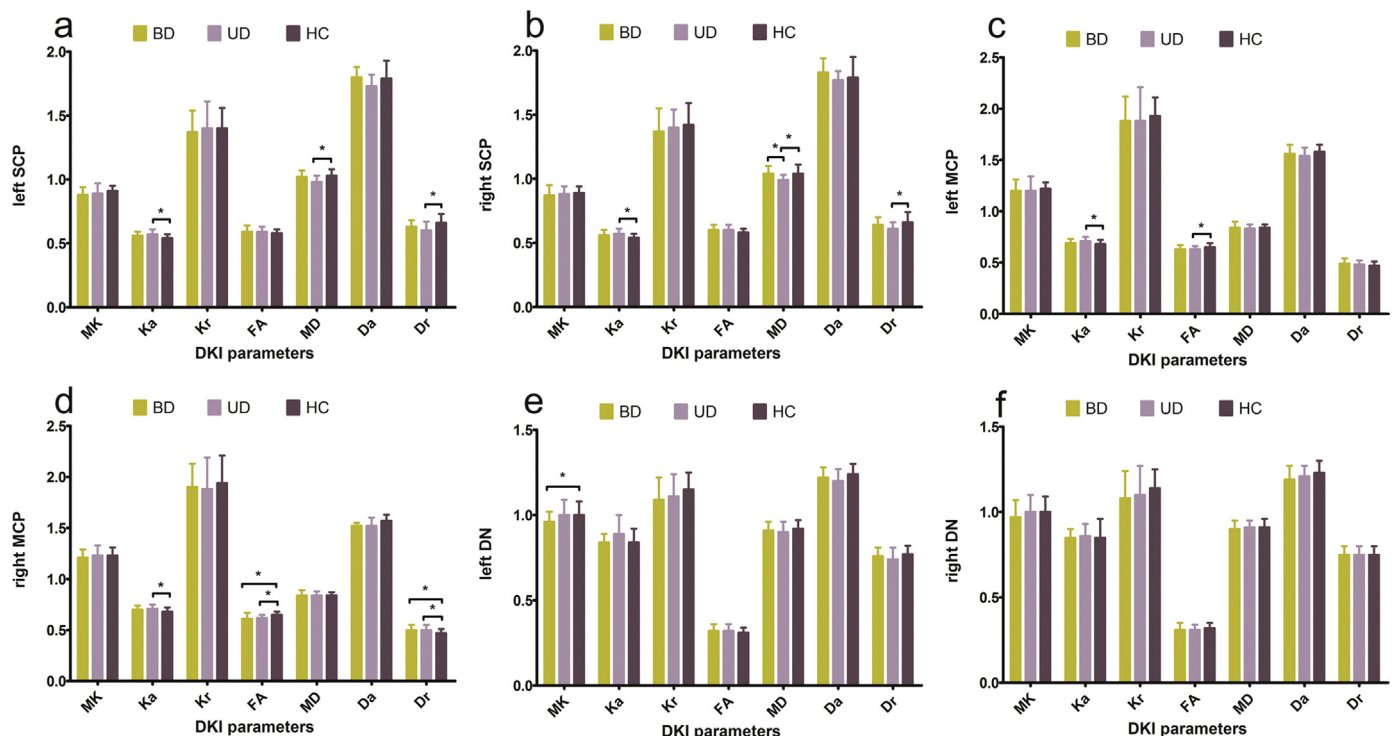
side	group				F-value	ANOVA P-value	multiple comparison P-value		
		BD(n=35)	UD(n=30)	HC(n=35)			BD vs UD	UD vs HC	BD vs HC
SCP									
MK	left	0.88(0.06)	0.89(0.08)	0.91(0.04)	2.397	0.096	1.000	0.457	0.115
	right	0.87(0.08)	0.88(0.06)	0.89(0.05)	1.435	0.243	1.000	1.000	0.281
Ka	left	0.56(0.03)	0.57(0.04)	0.54(0.03)	3.332	0.039	0.285	0.034*	0.892
	right	0.56(0.04)	0.57(0.04)	0.54(0.03)	3.804	0.025	0.743	0.027*	0.242
Kr	left	1.37(0.17)	1.40(0.21)	1.40(0.16)	0.404	0.669	1.000	1.000	1.000
	right	1.37(0.18)	1.40(0.14)	1.42(0.17)	1.022	0.363	1.000	1.000	0.468
FA	left	0.59(0.05)	0.59(0.04)	0.58(0.03)	0.161	0.851	1.000	1.000	1.000
	right	0.60(0.04)	0.60(0.04)	0.58(0.03)	1.586	0.209	1.000	0.712	0.279
MD	left	1.02(0.05)	0.98(0.05)	1.03(0.05)	5.813	0.004	0.061	0.003*	0.648
	right	1.04(0.06)	0.99(0.04)	1.04(0.07)	3.488	0.034	0.008*	0.023*	1.000
Da	left	1.80(0.08)	1.73(0.09)	1.79(0.14)	2.193	0.117	0.127	0.302	1.000
	right	1.83(0.11)	1.77(0.07)	1.79(0.16)	2.692	0.072	0.104	1.000	0.268
Dr	left	0.63(0.05)	0.60(0.07)	0.66(0.07)	5.264	0.007	0.357	0.006*	0.176
	right	0.64(0.06)	0.61(0.05)	0.66(0.08)	3.332	0.039	0.414	0.035*	0.612
MCP									
MK	left	1.20(0.11)	1.20(0.14)	1.22(0.06)	0.563	0.571	0.999	0.878	0.593
	right	1.21(0.08)	1.23(0.10)	1.23(0.08)	0.636	0.531	1.000	1.000	1.000
Ka	left	0.69(0.04)	0.71(0.04)	0.68(0.04)	4.874	0.009	0.081	0.008*	1.000
	right	0.70(0.04)	0.71(0.04)	0.68(0.04)	3.847	0.024	1.000	0.044*	0.089
Kr	left	1.88(0.24)	1.88(0.33)	1.93(0.18)	0.493	0.612	1.000	1.000	1.000
	right	1.90(0.23)	1.88(0.31)	1.94(0.27)	0.525	0.593	1.000	1.000	1.000
FA	left	0.63(0.04)	0.63(0.03)	0.65(0.04)	3.875	0.024	1.000	0.027*	0.204
	right	0.61(0.06)	0.62(0.03)	0.65(0.03)	7.782	0.001	1.000	0.020*	0.001*
MD	left	0.84(0.06)	0.83(0.04)	0.84(0.03)	0.189	0.828	1.000	1.000	1.000
	right	0.84(0.05)	0.84(0.04)	0.84(0.03)	0.112	0.894	1.000	0.971	0.967
Da	left	1.56(0.09)	1.54(0.08)	1.58(0.07)	2.295	0.106	0.932	0.113	0.647
	right	1.52(0.03)	1.52(0.08)	1.57(0.06)	2.974	0.055	1.000	0.212	0.084
Dr	left	0.49(0.05)	0.48(0.04)	0.47(0.04)	2.366	0.099	1.000	0.905	0.097
	right	0.50(0.05)	0.50(0.05)	0.47(0.04)	5.296	0.006	1.000	0.045*	0.012*
DN									
MK	left	0.96(0.06)	1.00(0.09)	1.00(0.08)	3.560	0.032	0.130	1.000	0.047*
	right	0.97(0.10)	1.00(0.10)	1.00(0.09)	1.551	0.217	0.737	1.000	0.273
Ka	left	0.84(0.05)	0.89(0.11)	0.84(0.08)	3.255	0.042	0.069	0.074	1.000
	right	0.85(0.05)	0.86(0.07)	0.85(0.11)	0.134	0.874	1.000	1.000	1.000
Kr	left	1.09(0.13)	1.11(0.13)	1.15(0.10)	2.429	0.093	1.000	0.523	0.102
	right	1.08(0.16)	1.10(0.17)	1.14(0.11)	2.340	0.101	1.000	0.578	0.110
FA	left	0.32(0.04)	0.32(0.04)	0.31(0.03)	0.221	0.802	1.000	1.000	1.000
	right	0.31(0.04)	0.31(0.03)	0.32(0.03)	0.695	0.501	1.000	1.000	0.865
MD	left	0.91(0.05)	0.90(0.06)	0.92(0.05)	1.971	0.144	0.933	0.155	0.849
	right	0.90(0.05)	0.91(0.04)	0.91(0.05)	1.971	0.144	1.000	1.000	0.553
Da	left	1.22(0.06)	1.20(0.07)	1.24(0.06)	2.270	0.070	0.764	0.070	0.573
	right	1.19(0.08)	1.21(0.06)	1.23(0.07)	2.596	0.079	0.843	1.000	0.074
Dr	left	0.76(0.05)	0.74(0.07)	0.77(0.05)	1.124	0.329	1.000	0.415	1.000
	right	0.75(0.05)	0.75(0.05)	0.75(0.05)	0.253	0.777	1.000	1.000	1.000

Diffusional kurtosis metrics estimates are reported as mean (standard deviation) in each brain region of interests in the cerebellum. One-way ANOVA with significant p-values in bold; a (*) indicates that the group difference remained significant after applying Bonferroni correction. DKI= diffusional kurtosis imaging. MK=mean kurtosis. KA= axial kurtosis. Kr= radial kurtosis. FA=fractional anisotropy. MD=mean diffusivity. Da=axial diffusivity. Dr= radial diffusivity. SCP= superior cerebellar peduncles. MCP= middle cerebellar peduncles. DN=dentate nuclei. BD=bipolar disorder. UD=unipolar depression. HC=healthy controls. The units for MD, Da and Dr are all $\mu\text{m}^2/\text{ms}$; MK, Ka and FA are dimensionless parameters.

cortex in patients with UD, which further support our findings (Guo et al., 2013b). Furthermore, we also found significant negative correlations between MD/Dr and illness duration in the right SCP in UD, suggesting that the duration of the illness itself was responsible for the microstructure impairment of this brain region. Taken together, the present microstructure changes in SCP provide novel evidence for structural damage in UD. We did not find any significant changes in SCP in BD, this suggests that SCP microstructure damage may be specific to UD rather than an overlapping feature between the two disorders. It would be a potential biomarkers for distinguishing the two disorders. However, no research, so far, has been reported these differences between BD and UD, thus further studies which include large samples are needed to confirm the role for the SCP in the two disorders.

We also observed decreased CBF in patient with UD compared with HC in the bilateral SCP. Gonul et al. found UD patients had decreased CBF perfusion ratios in the left cerebellum by single

photon emission computed tomography (Gonul et al., 2004), which is in agreement with our findings. However, these findings are somewhat contrary to a previous positron emission tomography (PET) study (Videbech et al., 2002) which showed increased blood flow in the cerebellum in UD. The inconsistency may be attributed to numerous factors. First, medication status could play a role in CBF variation. Davies J et al. reported a significantly decreased CBF after antidepressant in the right cerebellum (Davies et al., 2003). And Loeber RL et al. point out that antipsychotic treatment as well as affective state may produce an increase in cerebellar blood volume (Loeber et al., 2000). Second, different specific ROIs location may lead to different results. We observed the SCP, MCP and DN while the previously PET study observed the cerebellar hemisphere and vermis. Third, CBF varies in different episode. Kohn Y et al. reported CBF decreased in remitted patients in bilateral cerebellar regions when scans in long-term remission and immediately after treatment were compared



The units for MD, Da and Dr are all $\mu\text{m}^2/\text{ms}$; MK, Ka, Kr and FA are dimensionless parameters.

Fig. 4. a-f: group differences of the parameters generated from DKI. Fig. 4a-b: group differences of the DKI parameters in the left and right SCP respectively. Fig. 4c-d: group differences of the DKI parameters in the left and right MCP respectively. Fig. 4e-f: group differences of the DKI parameters in the left and right DN respectively. * $P < 0.05$.

Table 4

Comparison of the CBF from 3D ASL of cerebellum in patients with BD, UD and HC subjects.

side	group				F-value	ANOVA P-value	multiple comparison P-value		
		BD (n=35)	UD (n=30)	HC (n=35)			BD vs UD	UD vs HC	BD vs HC
SCP									
CBF	left	46.48(10.92)	43.75(7.58)	50.03(9.83)	3.684	0.028	0.743	0.028*	0.267
	right	47.14(10.35)	44.05(8.12)	50.07(10.82)	3.102	0.049	0.608	0.045*	0.513
MCP									
CBF	left	41.32(9.04)	39.52(6.18)	42.65(8.18)	1.345	0.264	1.000	0.311	1.000
	right	42.18(9.33)	41.77(7.96)	44.24(8.26)	0.956	0.387	1.000	0.680	0.775
DN									
CBF	left	47.38(10.44)	46.71(9.04)	53.28(10.72)	5.119	0.007	1.000	0.020*	0.021*
	right	51.56(12.05)	51.50(9.79)	55.82(10.49)	2.169	0.119	1.000	0.280	0.201

CBF generated from 3D ASL are reported as mean (standard deviation) in each brain region of interests in the cerebellum. One-way ANOVA with significant p -values in bold; a (*) indicates that the group difference remained significant after applying Bonferroni correction. CBF=cerebral blood flow. SCP=superior cerebellar peduncles. MCP=middle cerebellar peduncles. DN=dentate nuclei. BD=bipolar disorder. UD=unipolar depression. HC=healthy controls. The unit for CBF is ml/100 g/min.

(Kohn et al., 2008). However, the patients included in our study were all in depressive episode. Besides, when compared with PET, ASL provides similar quantitative CBF as PET (Heijtel et al., 2014; Schmid et al., 2015). Furthermore, unlike PET techniques, ASL technique has the advantage of not using radioactive sources or injected contrast agents, showed a higher longitudinal repeatability for regional perfusion measurements (Kilroy et al., 2014), allowing for frequent scanning, especially useful in long-term follow-up studies. In addition, differences in sample size, age range, age of depression onset, the comorbidities of the subjects, as well as differences in data acquisition and data preprocessing would lead to an inconsistent result. However, these results demonstrated that abnormal blood flow was existed in the SCP and thus affecting the function of this structure in UD patients. Further, Mikita et al. found the depressive symptoms were negatively associated with CBF change in the cerebellum (Mikita et al., 2015). Unfortunately, we didn't find any correlations between CBF and

HDRS-24 scores. Although we didn't find a significant decrease in CBF and DKI parameters in SCP in BD, the moderate changes in CBF might reflect changes in vascular and cellular function associated with neuronal recovery or degeneration for which MK, FA, and MD lack sensitivity (Grossman et al., 2013). Therefore, these findings of decreased CBF in the SCP suggest hypoperfusion in this structure may be pathophysiological important in depression. Further studies which include large samples and homogeneous subjects are needed to confirm the CBF changes in the two disorders.

The MCP forms the major connection from the pons to the cerebellum, relaying information from the forebrain. In the present study, we found decreased FA and increased Dr and Ka in the bilateral MCP in UD and decreased FA in the right MCP in BD. Decreased FA is reflective of an impaired directional coherence (Tha et al., 2013) and increased Dr is an index for myelin injury (Lin et al., 2012) of the brain microstructures. As revealed by the reports of autopsies and biopsies of various diseases of the brain

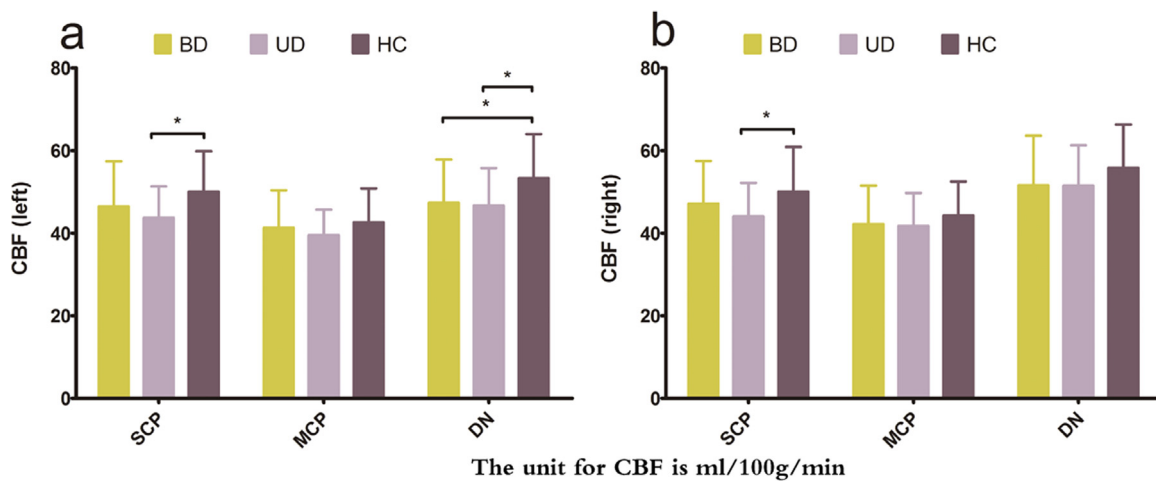


Fig. 5. a-b: group differences of CBF in the left and right SCP, MCP and DN respectively. * $P < 0.05$.

and experimental models, decreased FA correlates with histological changes, include larger axonal spacing, decrease in axon count, diameter and density, and myelin loss (Tha et al., 2013). Therefore, according to the above theory, the results of this study may likewise be associated with microstructural abnormalities in terms of the demyelination or myelin injury that leads to less diffusion restriction (Lin et al., 2012). In agreement with our findings, Bessette KL et al. found FA reductions in the bilateral MCP within the midbrain in UD patients (Bessette et al., 2014). Further, Lin WC et al. found decreased FA and increased Dr was correlated with depression (Lin et al., 2012). Similarly, Schneider-Gold C et al. found atrophy of MCP was correlated with depression (Schneider-Gold et al., 2015). Although lack of evidence of MCP changes in BD from the literatures, these findings all support the current results that microstructure impairment was existed both in BD and UD in that the patients with BD included in our study were all in a depressive episode. Taken together, our findings provide further evidence for the involvement of MCP impairment in the pathophysiology of BD and UD.

Another important finding in the present study is the significant decreased MK of the left DN in BD but not in UD. Higher MK value reflects more complex tissues microstructurally and restriction in the structure (Helpern et al., 2011) while lower MK value may suggest a loss of microstructural integrity in the region (Zhu et al., 2015). Therefore, our findings indicated that microstructural impairment was existed in the left DN in BD.

Postmortem studies of bipolar subjects showed abnormal reductions in neuronal and glial cell density in cerebral cortex in relation to controls (Rajkowska et al., 2001; Todtenkopf et al., 2005) which would result in MK decrease. It was further supported our findings as these structures (i.e. cerebral cortex and DN) are all the gray matters. In addition, we also observed CBF decrease in left DN in both BD and UD group. Loeber RL et al. found a positive correlation between depressive symptoms and mean cerebellar blood volume of the tonsils and left DN (Loeber et al., 2000). Unfortunately, we did not find a significant correlation between CBF and the clinical variables in DN in patients with either BD or UD. It has not, however, been possible to determine whether the CBF changes are a consequence or a cause of the microstructural findings. Taken together, the present decreased CBF in left DN was an overlapping pathophysiology between the two disorders. However, decreased MK in the left DN provides novel evidence for microstructural damage in BD and therefore may be a key neurobiological feature of BD.

Several limitations to this pilot study need to be acknowledged. (i) The number of participants in the present study was not large, although larger than in many previous studies. It is possible that subtle differences between groups would have been detected in a larger sample size. (ii) Parts of the patients included were under medication prior to MRI scanning. Furthermore, the medication varied, and the number of subjects was too limited to group them according to a specific type of drug. (iii) The ROIs on the area of the

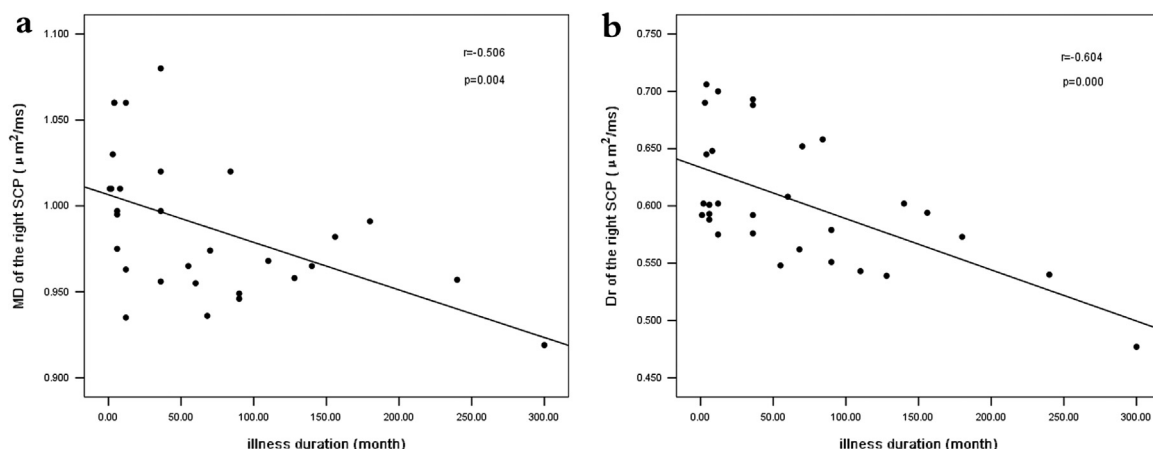


Fig. 6. a-b: Correlations between the clinical variables and measured DKI and 3D ASL parameters. Fig. 6a: Correlation between illness duration and MD in the right SCP in UD group. Fig. 6b: Correlation between illness duration and Dr in the right SCP in UD group.

SCP, MCP and DN were drew manually, and the reproducibility of measurements was unclear. However, all ROIs were drew by two of the authors, rater bias was prevented by blinding, and the inter-class correlation coefficients were 0.704–0.983. (iv) Because DKI demands high b-value diffusion weighted images, it is sensitive to noise and it has slight deformation in the basilar region. Consequently, the resolution of the acquired images is suboptimal to sustain sufficiently high signal-to-noise ratios and to minimize acquisition time. This may have led to partial volume effects, which could have reduced the sensitivity of the analysis. (v) In 3D ASL, only one post-labelling delay time (1,525 ms) in pCASL was used, which may have potential influences on the evaluation of cerebral flow in some cases. Besides, uncorrected maps in pCASL were used. However, to decrease the partial volume effects of pCASL acquisitions, a previous study acquired both uncorrected maps and maps corrected for partial volume effects, which yielded similar results, and CBF maps corrected for partial volume effects were not feasible for clinical use (Binnewijzend et al., 2013). (vi) Parts of the patients in our study were with chronic and severe mood disorder but unmedicated, it is difficult to generalize the results to the larger group of less severely ill patients with unipolar or bipolar depression. (vii) It has not been possible to determine whether our findings are a state biomarker or a trait biomarker for BD and UD since the patients included were all in depressive episodes. Studies using patients in remission from BD and UD would be helpful for finding steady consistent biomarkers to distinguish the two disorders. (viii) In the present study, we only investigate the cerebellar abnormalities in BD and UD, so that it can be further evaluated the prefrontal cortex and limbic system in the two disorders using DKI and ASL. (ix) Most of the results are post hoc. (x) The current study is a cross-sectional study, although the present patients with UD had no family history of BD, in the absence of longitudinal data we do not know whether some patients will later switch to BD.

5. Conclusions

In conclusion, our findings are the first to reveal the potentially important role for SCP, MCP and DN of cerebellum in BD and UD. Our results suggest that these two disorders may have overlaps in microstructural and functional abnormality in MCP and DN during the depressive period. Microstructural abnormality in SCP may be a key neurobiological feature of UD. Returning to the hypothesis posed at the beginning of this study, it is now possible to state that microstructural abnormalities and CBF changes of the cerebellum in prefrontal-thalamic-cerebellar circuitry play a key role in neurobiological process in patient with BD and UD.

Acknowledgments

The study was supported by grants from the National Natural Science Foundation of China (81501456, 81471650); Natural Science Foundation of Guangdong Province, China (2014A030313375); Planned Science and Technology Project of Guangdong Province, China (2014B020212022); Planned Science and Technology Project of Guangzhou, China (1563000653); Fundamental Research Funds for the Central Universities, China (21615476). The funding organizations play no further role in study design, data collection, analysis and interpretation and paper writing.

Appendix A. Supplementary material

Supplementary data associated with this article can be found in the online version at <http://dx.doi.org/10.1016/j.jad.2016.01.042>.

References

- Abe, O., Yamasue, H., Kasai, K., Yamada, H., Aoki, S., Inoue, H., Takei, K., Suga, M., Matsuo, K., Kato, T., Masutani, Y., Ohtomo, K., 2010. Voxel-based analyses of gray/white matter volume and diffusion tensor data in major depression. *Psychiatry research* 181, 64–70.
- Alsop, D.C., Detre, J.A., 1996. Reduced transit-time sensitivity in noninvasive magnetic resonance imaging of human cerebral blood flow. *Journal of cerebral blood flow and metabolism: official journal of the International Society of Cerebral Blood Flow and Metabolism* 16, 1236–1249.
- Ambrosi, E., Chiappponi, C., Sani, G., Manfredi, G., Piras, F., Caltagirone, C., Spalletta, G., 2016. White matter microstructural characteristics in Bipolar I and Bipolar II Disorder: A diffusion tensor imaging study. *Journal of affective disorders* 189, 176–183.
- Arnold, J.F., Zwiers, M.P., Fitzgerald, D.A., van Eijndhoven, P., Becker, E.S., Rinck, M., Fernandez, G., Speckens, A.E., Tendolkar, I., 2012. Fronto-limbic microstructure and structural connectivity in remission from major depression. *Psychiatry research* 204, 40–48.
- Bessette, K.L., Nave, A.M., Caprihan, A., Stevens, M.C., 2014. White matter abnormalities in adolescents with major depressive disorder. *Brain Imaging Behav* 8, 531–541.
- Binnewijzend, M.A.A., Kuijjer, J.P.A., Benedictus, M.R., van der Flier, W.M., Wink, A. M., Wattjes, M.P., van Berckel, B.N.M., Scheltens, P., Barkhof, F., 2013. Cerebral Blood Flow Measured with 3D Pseudocontinuous Arterial Spin-labeling MR Imaging in Alzheimer Disease and Mild Cognitive Impairment: A Marker for Disease Severity. *Radiology* 267, 221–230.
- Bonilha, L., Lee, C.Y., Jensen, J.H., Tabesh, A., Spampinato, M.V., Edwards, J.C., Bredt, J., Helpern, J.A., 2014. Altered Microstructure in Temporal Lobe Epilepsy: A Diffusional Kurtosis Imaging Study. *AJR Am J Neuroradiol*.
- Bowden, C.L., 2010. Diagnosis, treatment, and recovery maintenance in bipolar depression. *J Clin Psychiatry* 71, e01.
- Buckner, R.L., 2013. The cerebellum and cognitive function: 25 years of insight from anatomy and neuroimaging. *Neuron* 80, 807–815.
- Cai, Y., Liu, J., Zhang, L., Liao, M., Zhang, Y., Wang, L., Peng, H., He, Z., Li, Z., Li, W., Lu, S., Ding, Y., Li, L., 2015. Grey matter volume abnormalities in patients with bipolar I depressive disorder and unipolar depressive disorder: a voxel-based morphometry study. *Neurosci Bull* 31, 4–12.
- Chen, Y., Wang, C., Zhu, X., Tan, Y., Zhong, Y., 2015. Aberrant connectivity within the default mode network in first-episode, treatment-naïve major depressive disorder. *Journal of affective disorders* 183, 49–56.
- Cheung, M.M., Hui, E.S., Chan, K.C., Helpern, J.A., Qi, L., Wu, E.X., 2009. Does diffusion kurtosis imaging lead to better neural tissue characterization? A rodent brain maturation study. *NeuroImage* 45, 386–392.
- Davies, J., Lloyd, K.R., Jones, I.K., Barnes, A., Pilowsky, L.S., 2003. Changes in regional cerebral blood flow with venlafaxine in the treatment of major depression. *The American journal of psychiatry* 160, 374–376.
- Davis, J.A., Gamble, K.L., 2015. Synchronized Time Keeping is Key to Healthy Mood Regulation (Commentary on Landgraf et al.). *The European journal of neuroscience*.
- Gonul, A.S., Kula, M., Bilgin, A.G., Tutus, A., Oguz, A., 2004. The regional cerebral blood flow changes in major depressive disorder with and without psychotic features. *Progress in neuro-psychopharmacology & biological psychiatry* 28, 1015–1021.
- Grossman, E.J., Jensen, J.H., Babb, J.S., Chen, Q., Tabesh, A., Fieremans, E., Xia, D., Ingles, M., Grossman, R.I., 2013. Cognitive Impairment in Mild Traumatic Brain Injury: A Longitudinal Diffusional Kurtosis and Perfusion Imaging Study. *American Journal of Neuroradiology* 34, 951–957.
- Guo, W., Liu, F., Xue, Z., Gao, K., Liu, Z., Xiao, C., Chen, H., Zhao, J., 2013a. Abnormal resting-state cerebellar-cerebral functional connectivity in treatment-resistant depression and treatment sensitive depression. *Progress in neuro-psychopharmacology & biological psychiatry* 44, 51–57.
- Guo, W., Liu, F., Xue, Z., Gao, K., Liu, Z., Xiao, C., Chen, H., Zhao, J., 2013b. Abnormal resting-state cerebellar-cerebral functional connectivity in treatment-resistant depression and treatment sensitive depression. *Progress in neuro-psychopharmacology & biological psychiatry* 44, 51–57.
- Heijtel, D.F.R., Mutsaerts, H., Bakker, E., Schober, P., Stevens, M.F., Petersen, E.T., van Berckel, B.N.M., Majoe, C., Boos, J., van Osch, M.J.P., van Bavel, E., Boellaard, R., Lammertsma, A.A., Nederveen, A.J., 2014. Accuracy and precision of pseudo-continuous arterial spin labeling perfusion during baseline and hypercapnia: A head-to-head comparison with O-15 H2O positron emission tomography. *NeuroImage* 92, 182–192.
- Helpern, J.A., Adisetiyo, V., Falangola, M.F., Hu, C., Di Martino, A., Williams, K., Castellanos, F.X., Jensen, J.H., 2011. Preliminary evidence of altered gray and white matter microstructural development in the frontal lobe of adolescents with attention-deficit hyperactivity disorder: a diffusional kurtosis imaging study. *J Magn Reson Imaging* 33, 17–23.
- Honey, G.D., Pomarol-Clotet, E., Corlett, P.R., Honey, R.A., McKenna, P.J., Bullmore, E. T., Fletcher, P.C., 2005. Functional dysconnectivity in schizophrenia associated with attentional modulation of motor function. *Brain: a journal of neurology* 128, 2597–2611.
- Hui, E.S., Cheung, M.M., Qi, L., Wu, E.X., 2008. Towards better MR characterization of neural tissues using directional diffusion kurtosis analysis. *NeuroImage* 42, 122–134.
- Jarnum, H., Steffensen, E.G., Knutsson, L., Frund, E.T., Simonsen, C.W., Lundby-Christensen, S., Shankaranarayanan, A., Alsop, D.C., Jensen, F.T., Larsson, E.M.,

2010. Perfusion MRI of brain tumours: a comparative study of pseudo-continuous arterial spin labelling and dynamic susceptibility contrast imaging. *Neuroradiology* 52, 307–317.
- Jensen, J.H., Falangola, M.F., Hu, C., Tabesh, A., Rapalino, O., Lo, C., Helpern, J.A., 2011. Preliminary observations of increased diffusional kurtosis in human brain following recent cerebral infarction. *NMR Biomed* 24, 452–457.
- Jensen, J.H., Helpern, J.A., 2010. MRI quantification of non-Gaussian water diffusion by kurtosis analysis. *NMR Biomed* 23, 698–710.
- Jensen, J.H., Helpern, J.A., Ramani, A., Lu, H., Kaczynski, K., 2005. Diffusional kurtosis imaging: the quantification of non-gaussian water diffusion by means of magnetic resonance imaging. *Magn Reson Med* 53, 1432–1440.
- Kamagata, K., Tomiyama, H., Hatano, T., Motoi, Y., Abe, O., Shimoji, K., Kamiya, K., Suzuki, M., Hori, M., Yoshida, M., Hattori, N., Aoki, S., 2014. A preliminary diffusional kurtosis imaging study of Parkinson disease: comparison with conventional diffusion tensor imaging. *Neuroradiology* 56, 251–258.
- Kempton, M.J., Salvador, Z., Munro, M.R., Geddes, J.R., Simmons, A., Frangou, S., Williams, S.C., 2011. Structural neuroimaging studies in major depressive disorder. Meta-analysis and comparison with bipolar disorder. *Archives of general psychiatry* 68, 675–690.
- Kilroy, E., Apostolova, L., Liu, C., Yan, L., Ringman, J., Wang, D.J.J., 2014. Reliability of Two-Dimensional and Three-Dimensional Pseudo-Continuous Arterial Spin Labeling Perfusion MRI in Elderly Populations: Comparison With 15O-Water Positron Emission Tomography. *Journal of Magnetic Resonance Imaging* 39, 931–939.
- Kim, D., Cho, H.B., Dager, S.R., Yurgelun-Todd, D.A., Yoon, S., Lee, J.H., Lee, S.H., Lee, S., Renshaw, P.F., Lyoo, I.K., 2013. Posterior cerebellar vermal deficits in bipolar disorder. *Journal of affective disorders* 150, 499–506.
- Kohn, Y., Freedman, N., Lester, H., Krausz, Y., Chisin, R., Lerer, B., Bonne, O., 2008. Cerebral perfusion after a 2-year remission in major depression. *Int J Neuropsychopharmacol* 11, 837–843.
- Liang, M.-J., Zhou, Q., Yang, K.-R., Yang, X.-L., Fang, J., Chen, W.-L., Huang, Z., 2013. Identify Changes of Brain Regional Homogeneity in Bipolar Disorder and Unipolar Depression Using Resting-State fMRI. *PloS one*, 8.
- Lin, W.C., Chou, K.H., Chen, C.C., Huang, C.C., Chen, H.L., Lu, C.H., Li, S.H., Wang, Y.L., Cheng, Y.F., Lin, C.P., 2012. White matter abnormalities correlating with memory and depression in heroin users under methadone maintenance treatment. *PloS one* 7, e33809.
- Loeber, R.L., Gruber, S.A., Yurgelun-Todd, D.A., 2000. Cerebellar blood volume in bipolar disorder: relationship to symptoms and medication. *Society for Neuroscience Abstracts* 26, 96.
- Lu, H., Jensen, J.H., Ramani, A., Helpern, J.A., 2006. Three-dimensional characterization of non-gaussian water diffusion in humans using diffusion kurtosis imaging. *NMR Biomed* 19, 236–247.
- Machino, A., Kunisato, Y., Matsumoto, T., Yoshimura, S., Ueda, K., Yamawaki, Y., Okada, G., Okamoto, Y., Yamawaki, S., 2014. Possible involvement of rumination in gray matter abnormalities in persistent symptoms of major depression: an exploratory magnetic resonance imaging voxel-based morphometry study. *Journal of affective disorders* 168, 229–235.
- McKenna, B.S., Sutherland, A.N., Legenkaya, A.P., Eyler, L.T., 2014. Abnormalities of brain response during encoding into verbal working memory among euthymic patients with bipolar disorder. *Bipolar disorders* 16, 289–299.
- Mikita, N., Mehta, M.A., Zelaya, F.O., Stringaris, A., 2015. Using arterial spin labeling to examine mood states in youth. *Brain and Behavior*, 5.
- Okugawa, G., Nobuhara, K., Minami, T., Takase, K., Sugimoto, T., Saito, Y., Yoshimura, M., Kinoshita, T., 2006. Neural disorganization in the superior cerebellar peduncle and cognitive abnormality in patients with schizophrenia: a diffusion tensor imaging study. *Progress in neuro-psychopharmacology & biological psychiatry* 30, 1408–1412.
- Parker, K.L., Andreasen, N.C., Liu, D., Freeman, J.H., O'Leary, D.S., 2013. Eyeblink conditioning in unmedicated schizophrenia patients: a positron emission tomography study. *Psychiatry research* 214, 402–409.
- Rajkowska, G., Halaris, A., Selemion, L.D., 2001. Reductions in neuronal and glial density characterize the dorsolateral prefrontal cortex in bipolar disorder. *Biological psychiatry* 49, 741–752.
- Rapoport, M., van Reekum, R., Mayberg, H., 2000. The role of the cerebellum in cognition and behavior: a selective review. *The Journal of neuropsychiatry and clinical neurosciences* 12, 193–198.
- Redlich, R., Dohm, K., Grottegerd, D., Opel, N., Zwitslerlood, P., Heindel, W., Arot, V., Kugel, H., Dannlowski, U., 2015. Reward Processing in Unipolar and Bipolar Depression: A Functional MRI Study. *Neuropsychopharmacology: official publication of the American College of Neuropsychopharmacology*.
- Rusch, N., Spoletni, I., Wilke, M., Bria, P., Di Paola, M., Di Iulio, F., Martinotti, G., Caltagirone, C., Spalletta, G., 2007. Prefrontal-thalamic-cerebellar gray matter networks and executive functioning in schizophrenia. *Schizophrenia research* 93, 79–89.
- Sasayama, D., Hori, H., Teraishi, T., Hattori, K., Ota, M., Matsuo, J., Kawamoto, Y., Kinoshita, Y., Hashikura, M., Koga, N., Okamoto, N., Sakamoto, K., Higuchi, T., Amano, N., Kunugi, H., 2011. Difference in Temperament and Character Inventory scores between depressed patients with bipolar II and unipolar major depressive disorders. *Journal of affective disorders* 132, 319–324.
- Schmidmann, J.D., 2004. Disorders of the cerebellum: ataxia, dysmetria of thought, and the cerebellar cognitive affective syndrome. *The Journal of neuropsychiatry and clinical neurosciences* 16, 367–378.
- Schmid, S., Heijtel, D.F.R., Mutsaerts, H.J.M.M., Boellaard, R., Lammertsma, A.A., Nederveen, A.J., van Osch, M.J.P., 2015. Comparison of velocity- and acceleration-selective arterial spin labeling with O-15 H2O positron emission tomography. *Journal of Cerebral Blood Flow and Metabolism* 35, 1296–1303.
- Schneider-Gold, C., Bellenberg, B., Prehn, C., Krogias, C., Schneider, R., Klein, J., Gold, R., Lukas, C., 2015. Cortical and Subcortical Grey and White Matter Atrophy in Myotonic Dystrophies Type 1 and 2 Is Associated with Cognitive Impairment, Depression and Daytime Sleepiness. *PloS one* 10, e0130352.
- Song, S.K., Sun, S.W., Ramsbottom, M.J., Chang, C., Russell, J., Cross, A.H., 2002. Dysmyelination revealed through MRI as increased radial (but unchanged axial) diffusion of water. *NeuroImage* 17, 1429–1436.
- Tha, K.K., Terae, S., Nakagawa, S., Inoue, T., Kitagawa, N., Kako, Y., Nakato, Y., Akter Popy, K., Fujima, N., Zaitsu, Y., Yoshida, D., Ito, Y.M., Miyamoto, T., Koyama, T., Shirato, H., 2013. Impaired integrity of the brain parenchyma in non-geriatric patients with major depressive disorder revealed by diffusion tensor imaging. *Psychiatry research* 212, 208–215.
- Todtenkopf, M.S., Vincent, S.L., Benes, F.M., 2005. A cross-study meta-analysis and three-dimensional comparison of cell counting in the anterior cingulate cortex of schizophrenia and bipolar brain. *Schizophrenia research* 73, 79–89.
- Veraart, J., Poot, D.H., Van Hecke, W., Blockx, I., Van der Linden, A., Verhoeve, M., Sijbers, J., 2011. More accurate estimation of diffusion tensor parameters using diffusion Kurtosis imaging. *Magn Reson Med* 65, 138–145.
- Videbech, P., Ravnkilde, B., Pedersen, T.H., Hartvig, H., Egander, A., Clemmensen, K., Rasmussen, N.A., Andersen, F., Gjedde, A., Rosenberg, R., 2002. The Danish PET/depression project: clinical symptoms and cerebral blood flow. A regions-of-interest analysis. *Acta psychiatrica Scandinavica* 106, 35–44.
- Wang, J., Zhang, Y., Wolf, R.L., Roc, A.C., Alsop, D.C., Detre, J.A., 2005. Amplitude-modulated continuous arterial spin-labeling 3.0-T perfusion MR imaging with a single coil: feasibility study. *Radiology* 235, 218–228.
- Wang, Y., Zhong, S., Jia, Y., Zhou, Z., Wang, B., Pan, J., Huang, L., 2015a. Interhemispheric resting state functional connectivity abnormalities in unipolar depression and bipolar depression. *Bipolar disorders* 17, 486–495.
- Wang, Y., Zhong, S., Jia, Y., Zhou, Z., Zhou, Q., Huang, L., 2015b. Reduced interhemispheric resting-state functional connectivity in unmedicated bipolar II disorder. *Acta psychiatrica Scandinavica*.
- Wu, B., Lou, X., Wu, X., Ma, L., 2014. Intra- and interscanner reliability and reproducibility of 3D whole-brain pseudo-continuous arterial spin-labeling MR perfusion at 3T. *Journal of magnetic resonance imaging: JMRI* 39, 402–409.
- Xueying, L., Zhongping, Z., Zhoushe, Z., Li, G., Yongjin, T., Changzheng, S., Zhifeng, Z., Peihao, C., Hao, X., Li, H., 2015. Investigation of Apparent Diffusion Coefficient from Ultra-high b-Values in Parkinson's Disease. *European Radiology* 25, 2593–2600.
- Zhu, J., Zhuo, C., Qin, W., Wang, D., Ma, X., Zhou, Y., Yu, C., 2015. Performances of diffusion kurtosis imaging and diffusion tensor imaging in detecting white matter abnormality in schizophrenia. *NeuroImage: Clinical* 7, 170–176.